

CrystEngComm

Accepted Manuscript



This is an *Accepted Manuscript*, which has been through the Royal Society of Chemistry peer review process and has been accepted for publication.

Accepted Manuscripts are published online shortly after acceptance, before technical editing, formatting and proof reading. Using this free service, authors can make their results available to the community, in citable form, before we publish the edited article. We will replace this *Accepted Manuscript* with the edited and formatted *Advance Article* as soon as it is available.

You can find more information about *Accepted Manuscripts* in the [Information for Authors](#).

Please note that technical editing may introduce minor changes to the text and/or graphics, which may alter content. The journal's standard [Terms & Conditions](#) and the [Ethical guidelines](#) still apply. In no event shall the Royal Society of Chemistry be held responsible for any errors or omissions in this *Accepted Manuscript* or any consequences arising from the use of any information it contains.

Facile Fabrication of ZnO:S/ZnO Hetero-Nanostructures and Their Electronic Structure Investigation by Electron Energy-Loss Spectroscopy

*L. L. Wu,^{a,b} and X. T. Zhang,^{*b}*

^a Center for Engineering Training and Basic Experimentation, Heilongjiang University of Science and Technology, Harbin 150022, P. R. China

^b Key Laboratory for Photonic and Electronic Bandgap Materials, Ministry of Education, School of Physics and Electronic Engineering, Harbin Normal University, Harbin 150025, P. R. China

ABSTRACT Asymmetric ZnO:S/ZnO hetero-nanostructures with well-defined morphology were synthesized in a one-step gas phase condensation process. The as-synthesized products were systematically characterized by transmission electron microscopy. On the observations, a growth mechanism of the complicated hetero-nanostructures is suggested. The facile synthetic route to prepare these ZnO:S/ZnO hetero-nanostructures offers a possibility to satisfy the special needs in optoelectronic applications. The electronic structures of the hetero-nanostructures were investigated by electron energy-loss spectroscopy. Both the common features and the differences between the pure ZnO and S-doped ZnO sections are discussed. These features might provide a new test routine for sulfur implantation and be useful generally in the control, manipulation, transfer, and harvesting of UV light for ZnO.

KEYWORDS: Hetero-nanostructures; Synthesis; ZnO; Doping; Electron Energy-Loss Spectroscopy.

* Corresponding author: E-mail:xtzhangzhang@hotmail.com

Introduction

In the burgeoning field of nanotechnology, rational design and controlling the shape, size, and structure of nanomaterials is the essential aspect. Studies on new physical properties and applications of nanomaterials and nanostructures are possible only when nanostructured materials are made available with desired size, morphology, crystal and microstructure and chemical composition. Especially, growth control of inorganic nanomaterials is of fundamental importance in an extremely broad range of potential applications from nanoscale electronics and optics, to nanobiological systems and nanomedicine, to new materials.¹⁻³ Currently, hetero-nanostructures consisting of two or more components with controlled structural characteristics (including morphology, dimensionality, surface architectures, and crystal structures) have been attracting much attention.⁴ The novel and extraordinary properties of hetero-nanostructures outperform those of the individual components, and will not only satisfy everlasting human curiosity, but also promise new advancement in technology. For example, branched hetero-nanostructures are envisaged to be ideal model systems for energy band engineering.⁵⁻⁷ Direct fabrication of branched hetero-nanostructures is a significant challenge, and becomes a target for material researchers.

Zinc oxide is an important semiconductor material with a direct band gap of 3.37 eV and a large exciton binding energy of 60 meV. It has been recognized as one of the candidates for shortwave length optoelectronic device application. Thus many trials to establish a bandgap control of ZnO have been done. From this viewpoint, the

substitution of anions or cations by isoelectronic impurities is important. Extensive research on the fabrication of cation doped ZnO nanostructures have been done during the past few years.⁸⁻¹³ Recently, anion doping in ZnO, especially replacing oxygen by sulfur, has been reported.¹⁴⁻¹⁷ Due to a similar structure of the electronic shell, oxygen has many physical and chemical properties similar to those of sulfur. S-doping in ZnO is therefore expected to set the band gap in a wide energy range with low fraction of S.¹⁸⁻²⁰ In addition, the modification of the electrical and optical properties of ZnO might be possible due to the size difference between S and O ($r_s/r_o=1.3$).¹⁶

It is well recognized that the research on electronic structure can provide important information about the properties of materials and give an insight into the possible underlying mechanism of the observed unique performances of materials. By combining the crystallographic and chemical information provided by transmission electron microscopy, electron energy loss spectroscopy (EELS) has been widely used for studying the electronic structure of nanomaterials. The interactions of fast electrons with the specimen result in electrons being excited into unoccupied energy levels within the conduction band, as well as collective excitation of valance electrons (plasmon). In the low-loss region (up to ~50 eV), interband transitions and volume and surface plasma peaks are observed and can provide information about electronic structure such as the band-gap width, electronic density of states, and dielectric coefficient. With greater energy losses, ionization edges occur due to the core electrons being excited within the valence band and then entering the empty states of conduction bands.²¹⁻²⁴

In this study, asymmetric ZnO:S/ZnO branched hetero-nanostructures consisted of two parts: S doped ZnO trunk and pure ZnO branch are reported. A simple and safe self-assembly growth provides an effective approach for the fabrication of these branched hetero-nanostructures. The EELS spectra of as-synthesized nanostructures are also investigated.

Experimental Section

Synthesis. The ZnO:S/ZnO hetero-nanostructures were synthesized via a one-step thermal evaporation approach. It was carried out in a horizontal tube furnace through a fully controlled chemical vapor deposition (CVD) process. Commercial Zn and S powders were mixed in a mass ratio of 1 to 2, ground and then loaded on an alumina boat, and positioned at the center of the furnace, while Si (100) substrates coated with zinc foil (~1 mm in thickness) were placed downstream to collect the products. Prior to heating, the furnace chamber was first evacuated to 10 Pa and then high-purity Ar gas was kept flowing through the tube. Then the furnace was heated to 600 °C and held at this temperature for 10 mins. During the whole growth, Ar was used as a carrier gas at a constant flow rate and pressure: 100 sccm and 100 Pa. After that, the furnace was naturally cooled down to room temperature.

Measurement. The as-synthesized products together with the substrate were directly transferred into the instrument chamber for scanning electron microscopy (SEM, Hitachi, S4800), without destroying the original nature of the products on the substrate. The crystallinity and detailed structure of the products were further characterized by transmission electron microscope (TEM; FEI, Tecnai F20) equipped

with energy-dispersive X-ray spectroscopy (EDS), selected area electron diffraction (SAED). EELS spectra were acquired with 200 kV incident electrons from a FEI Tecnai F20 field-emission HRTEM. The energy resolution of the spectra was determined by measuring the full width at half-maximum (FWHM) of the zero loss peak, which was typically close to 0.8 eV. All of the EELS spectra were calibrated using the zero loss peak position.

Results and Discussion

The low magnification SEM image shown in Figure 1(a) gives the general morphology of the as-synthesized products. A large quantity of branched architectures with the length in range from several to tens of micrometers are clearly observed over the entire substrate. The branched architectures compose of a long trunk and three type of small branches decorated around the trunk in their own manner. The diameter of trunks is about 100 nm, larger than that of the branches. Typical SEM images in high magnification shown in Figure 1(b) and (c) display the orientation relationship of the branches. Two type of the branches huddle on either side of the trunk in a common plane. They are oriented at an angle of 60° or 120° with respect to the trunk, as shown in Figure 1(b). The length of the two type of branches is about 270 nm. Their diameter is about 50 nm. As shown in Figure 1(c), the third type of branches is perpendicular to the common plane of the former two and the trunk. When zoomed-in, this type of branches seems not to separate from each other completely. Their diameter and length are slightly larger than those of the first type.

To obtain detailed information about composition and microstructure, the branched architectures are further investigated by TEM, SAED, and EDS. Figure 2(a) shows the top view image of the branched architectures with the incident electron beam parallel to the growth direction of the third type of branches. Figure 2(b) shows the EDS spectra taken from the trunk and branches. The EDS spectra reveals that the trunk mainly consist of Zn, O and a very small amount of S. In contrast, the three type of branches all consist of Zn and O only. The Cu signals in EDS profile come from the TEM grid. A similar composition is also obtained by the EDS analyses performed on tens of other branched architectures. Further quantitative analysis shows that the atomic ratio of Zn:O is nearly 1:1, indicating that the trunk is S-doped ZnO, and the branches are pure ZnO. The SAED patterns taken from the two regions enclosed by rectangular in Figure 2(a) are shown in Figure 2(c) and (d), respectively. They are well indexed to the $[1\bar{2}1\bar{3}]$ and $[2\bar{1}\bar{1}0]$ zone axis of hexagonal close-packed structure, suggesting that the growth of the trunk and the former two type of branches occur along the $\langle 1\bar{2}12 \rangle$ and $\langle 0002 \rangle$ direction. Figure 2(e) is the corresponding HRTEM image of the trunk. It shows the perfect crystal lattice of wurtzite structure and the growth direction of the trunk, which is consistent with the SAED pattern in Figure 2(c). Figure 2(f) is the HRTEM image of the branch. It presents the clearly resolved interplanar distance of 0.26 nm along the growth direction of the branch, corresponding to the d-space of the (0002) plane in the wurtzite structure of ZnO.

How are the complicated branched hetero-nanostructures formed? Taking all the previous observations into account, the formation of these complicated branched

hetero-nanostructures may be realized in an unique hierarchical self-assembly process, though it is still not completely clear what exactly happened during the growth. It is believed that the S-doped ZnO trunks were first achieved in the experiment because of their larger diameter than that of the branches. The oxygen species likely originated from the trace remnant of oxygen that was not eliminated completely by flushing with Ar gas and/or the leakage of the reaction chamber during heating. Surface of the zinc foil on silicon substrate was oxidized, and served as the template for the growth of S-doped ZnO trunks. The non-c axis oriented growth of these S-doped ZnO trunks should be due to the effect of sulfur dopant on surface energy. As we known, {0001} faces are the highest-energy low-index planes for wurtzite crystal, so pure ZnO nanostructures tend to grow along the c-axis because of the lower energy. While with dopants, this growth habit would be changed because of the impact of impurities on surface energy.²⁵⁻²⁷ After the sulfur in precursor powder had been consumed completely, the third type of pure ZnO branches began to epitaxially grow perpendicular to the trunks in a line, and the former two type of branches subsequently grew in the intervals of the third type of branches, eventually forming the complicated ZnO:S/ZnO hetero-nanostructures. In S-doped ZnO trunks, sulfur implantation might introduce lattice defects, which have moved out the crystal structure during the growth process of trunks. These defects and the steps on the surface of trunks could provide the nucleation sites for the branches growth. In crystallography, the former two type of branches have a epitaxial relationship with trunks on the {01 $\bar{1}$ 0} plane, and have a twin relationship with each other about the

$\{\bar{1}2\bar{1}2\}$ plane. The growth direction of the third type of branches should be $\langle\bar{1}2\bar{1}3\rangle$. The exact growth mechanism of these complicated hetero-nanostructures undoubtedly needs further studies.

The electronic structures of the ZnO:S/ZnO hetero-nanostructures have been thoroughly investigated using electron energy-loss measurements in a transmission electron microscope. First, we focus on the low-loss energy spectra. Figure 3(a) shows a comparison of low-loss EELS spectra acquired from the ZnO:S trunk and pure ZnO branches. The spectra were aligned and normalized to the dominant peak with zero-loss peak removed. They are quite similar in their general structure, and both consist of a dominant bulk plasmon peak (18.9 eV) together with a broad and relatively weak right shoulder at 36.9 eV. According to the results of Hengehold et al. and Zhang et al., the right shoulder at 36.9 eV is mainly identified as the interband transition from the O 2s state to Zn 3p.^{28,29} Besides the right shoulder, a left shoulder is conspicuously observed in the low-loss EELS spectrum of the ZnO:S trunk. While it is rather weak and obscure in the low-loss EELS spectrum of the pure ZnO branches, just like the most cases observed in ZnO bulk.^{30,31} The peak features of this shoulder are magnified by performing a second-order differentiation of the loss function, as shown in Figure 3(b). The peak position is located at 5.56 eV. It is documented as the interband transition from the O 2p to Zn 3s.^{28,32} The difference in peak features between the low-loss EELS spectrum of the ZnO:S trunk and pure ZnO branches in Figure 3(a) might be caused by the implantation of sulfur. The

substituting of oxygen atom by sulfur would introduce the interband transition of S 3p to Zn 3s and contribute to the related surface guided modes.^{31,33}

In addition to the low-loss energy spectra, the spectra in the higher energy-loss region were also investigated. The Fourier-ratio deconvoluted experimental O K-edges acquired from the ZnO:S trunk and pure ZnO branches are shown in Figure 4. The two O-K spectra are obvious different in the edge shape, especially near the 544 eV. Since the energy-loss near-edge structure is sensitive to the surrounding atomic species, the difference in the edge shape might stem from the different chemical environment around oxygen atoms, which is induced by sulfur implantation.^{34,35} If this notion is correct, this feature would provide a new test routine of sulfur implantation. According to Hofer et al., the L₂₃ edge of zinc in ZnO and ZnS shows a similar behavior.³⁶ Figure 5 shows the Fourier-ratio deconvoluted experimental Zn L-edges acquired from the ZnO:S trunk and pure ZnO branches. The L₂ and L₃ edges of zinc can be clearly identified. They present the similar features, giving the no information of sulfur implantation.

Conclusions

In conclusion, asymmetric ZnO:S/ZnO branched hetero-nanostructures were synthesized by a simplified gas phase condensation process. A possible growth mechanism is proposed to explain the nanostructure formation. Although the detailed growth mechanism requires more systematic investigations, this facile method might be useful for the fabrication of nanoscale building blocks of arbitrary dimensions, morphologies, and materials of increasing complexity, especially branched

hetero-nanostructures. The synthesis strategy might be applied to other functional materials. The electronic structures of the ZnO:S/ZnO hetero-nanostructures have been investigated by EELS. The difference in the spectrum shape of low-loss and O K-edges spectra might stem from the sulfur implantation, and would provide a new test routine for sulfur implantation.

Acknowledgements

This work was partially supported by the Natural Science Foundation of China (No. 61154001), Natural Science Foundation of Heilongjiang Province for Returned Chinese Scholars (LC2013C17), Program for New Century Excellent Talents In Heilongjiang Provincial University (NCET) and Institution of Higher Education.

References:

1. L. Shi, Y. M. Xu, and Q. Li, *Nanoscale*, 2010, **2**, 2104-8.
2. L. Shi, C. J. Pei, Y. M. Xu, and Q. Li, *J. Am. Chem. Soc.*, 2011, **133**, 10328-31.
3. L. Shi, and Y. M. Dai, *J. Mater. Chem. A*, 2013, **1**, 12981-6.
4. X. S. Fang, Y. Bando, U. K. Gautam, T. Y. Zhai, S. Gradecak, and D. Golberg, *J. Mater. Chem.*, 2009, **19**, 5683-9.
5. S. B. Zhu, L. M. Shan, X. Tian, X. Y. Zheng, D. Sun, X. B. Liu, L. Wang, and Z. W. Zhou, *Ceram. Int.*, **40**, 11663-70.
6. J. Lee, H. S. Yang, N. S. Lee, O. Kwon, H. Y. Shin, S. Yoon, J. M. Baik, Y. S. Seo, and M. H. Kim, *Crystengcomm.*, 2013, **15**, 2367-71.
7. M. Devika, N. K. Reddy, A. Pevzner, and F. Patolsky, *Chemphyschem*, 2010, **11**, 809-14.
8. M. J. Zhou, H. J. Zhu, Y. Jiao, Y. Y. Rao, S. Hark, Y. Liu, L. M. Peng, and Q. Li, *J. Phys. Chem. C*, 2009, **113**, 8945-7.
9. X. T. Zhang, Y. C. Liu, J. G. Ma, Y. M. Lu, D. Z. Shen, W. Xu, G. Z. Zhong, and X. W. Fan, *Chin. Phys. Lett.*, 2003, **20**, 401-3.
10. H. Pan, Y. W. Zhu, H. Sun, Y. P. Feng, C. H. Sow, and J. Y. Lin, *Nanotechnology*, 2006, **17**, 5096-100.
11. J. Nomoto, T. Miyata, and T. Minami, *J. Vac. Sci. Technol. A*, 2009, **27**, 1001-5.
12. Y. Liang, X. T. Zhang, L. Qin, E. Zhang, H. Gao, and Z. G. Zhang, *J. Phys. Chem. B*, 2006, **110**, 21593-5.
13. H. Gao, H. Ji, X. Zhang, H. Lu, and Y. Liang, *J. Vac. Sci. Technol. B*, 2008, **26**, 585-8.
14. S. G. Hussain, D. Liu, X. Huang, K. M. Sulieman, J. Liu, H. Liu, and R. U. Rasool, *J. Phys. D*, 2007, **40**, 7662-8.

15. S. G. Hussain, D. Liu, X. Huang, S. Ali, and M. H. Sayyad, *J. Phys. Chem. C*, 2008, **112**, 11162-8.
16. S. G. Hussain, D. M. Liu, X. T. Huang, K. M. Sulieman, J. P. Liu, H. R. Liu, and A. N. A. Alla, *Smart Mater. Struct.*, 2007, **16**, 1736-41.
17. G. Z. Shen, J. H. Cho, J. K. Yoo, G. C. Yi, and C. J. Lee, *J. Phys. Chem. B*, 2005, **109**, 5491-6.
18. B. Y. Geng, G. Z. Wang, Z. Jiang, T. Xie, S. H. Sun, G. W. Meng, and L. D. Zhang, *Appl. Phys. Lett.*, 2003, **82**, 4791-3.
19. B. K. Meyer, A. Polity, B. Farangis, Y. He, D. Hasselkamp, T. Kramer, and C. Wang, *Appl. Phys. Lett.*, 2004, **85**, 4929-31.
20. S. Locmelis, C. Bruenig, M. Binnewies, A. Boerger, K. D. Becker, T. Homann, and T. Bredow, *J. Mater. Sci.*, 2007, **42**, 1965-71.
21. R. F. Egerton, *Electron Energy-Loss Spectroscopy in the Electron Microscope*, second ed. 1986, Plenum Press, New York.
22. V. J. Keast, *J. Electron. Spectrosc. Relat. Phenom.*, 2005, **143**, 97-104.
23. Y. Ding and Z. L. Wang, *J. Electron Microsc.*, 2005, **54**, 287-91.
24. H. J. Morales-Rodriguez and F. Espinosa-Magana, *Micron*, 2012, **43**, 177-82.
25. H. J. Fan, B. Fuhrmann, R. Scholz, C. Himcinschi, A. Berger, H. Leipner, A. Dadgar, A. Krost, S. Christiansen, U. Gosele, and M. Zacharias, *Nanotechnology*, 2006, **17**, S231-9.
26. H. J. Fan, A. S. Barnard, and M. Zacharias, *Appl. Phys. Lett.*, 2007, **90**, 143116.
27. Z. L. Wang, *J. Phys.: Condens. Matter*, 2004, **16**, R829-58.
28. Z. H. Zhang, X. Y. Qi, J. K. Han, and X. F. Duan, *Micron*, 2006, **37**, 229-33.
29. R. L. Hengehold, R. J. Almassy, and F. L. Pedrotti, *Phys. Rev. B*, 1970, **1**, 4784.
30. M. R. S. Huang, R. Erni, H. Y. Lin, R. C. Wang, and C. P. Liu, *Phys. Rev. B*, 2011.

84, 155203.

31. K. Dileep and R. Datta, *J. Alloys Compd.*, 2014, **586**, 499-506.

32. C. T. Wu, M. W. Chu, C. P. Liu, K. H. Chen, L. C. Chen, C. W. Chen, and C. H. Chen, *Plasmonics*, 2012, **7**, 123-30.

33. Z. H. Zhang, M. He, and X. F. Duan, *Chin. Phys. Lett.*, 2009, **26**, 066104.

34. X. Wang, F. Song, Q. Chen, T. Wang, J. Wang, P. Liu, M. Shen, J. Wan, G. Wang, and J. B. Xu, *J. Am. Chem. Soc.*, 2010, **132**, 6492-7.

35. T. Mizoguchi, M. Yoshiya, J. Li, F. Oba, I. Tanaka, and H. Adachi, *Ultramicroscopy*, 2001, **86**, 363-70.

36. F. Hofer and P. Golob, *Ultramicroscopy*, 1987, **21**, 379-83.

Figure Captions:

Figure 1 (a) Low magnification SEM image; (b) High magnification SEM image; (c) High magnification SEM image of the ZnO:S/ZnO hetero-nanostructures.

Figures 2 (a) Low-magnification TEM image; (b) EDX spectra of the ZnO:S/ZnO hetero-nanostructures; (c) SAED pattern in the $[1\bar{2}1\bar{3}]$ zone axis of the ZnO:S trunk; (d) SAED pattern in the $[2\bar{1}\bar{1}0]$ zone axis of pure ZnO branches; (e) HRTEM image corresponding to (c); (f) HRTEM image corresponding to (d).

Figure 3 (a) Low-loss EELS spectra acquired from the ZnO:S trunk and pure ZnO branches; (b) the corresponding second derivatives of the loss function.

Figure 4 Near-edge fine structures for the O K-edges acquired from the ZnO:S trunk and pure ZnO branches.

Figure 5 Near-edge fine structures for the Zn L-edges acquired from the ZnO:S trunk and pure ZnO branches.

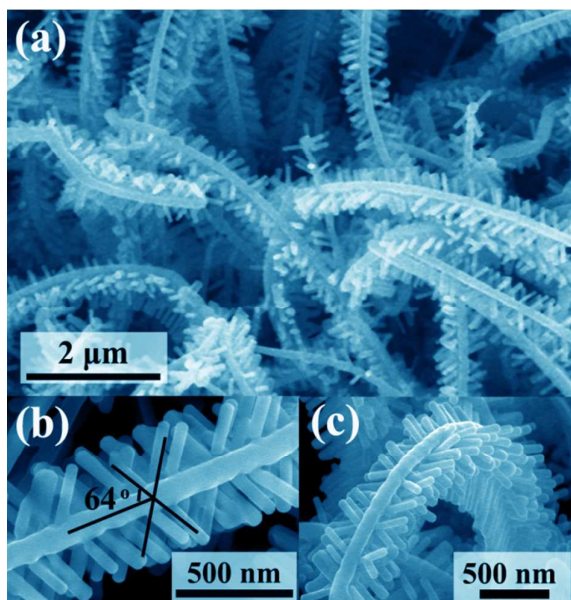


Figure 1 by L. L. Wu, et al.

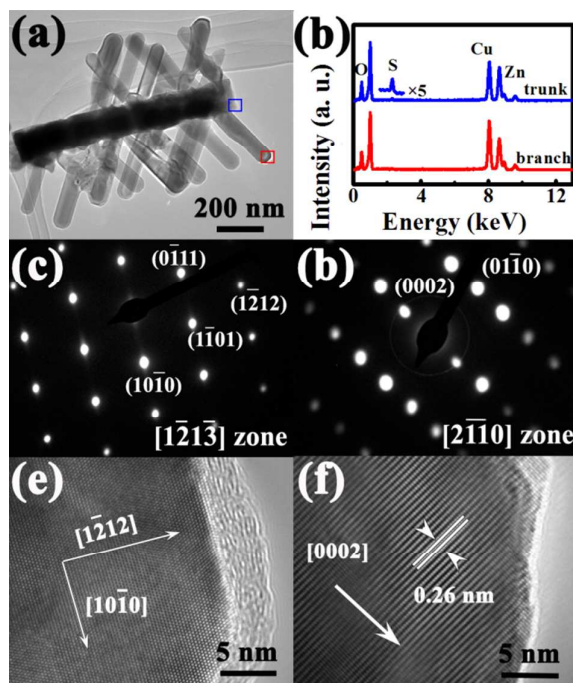


Figure 2 by L. L. Wu, et al.

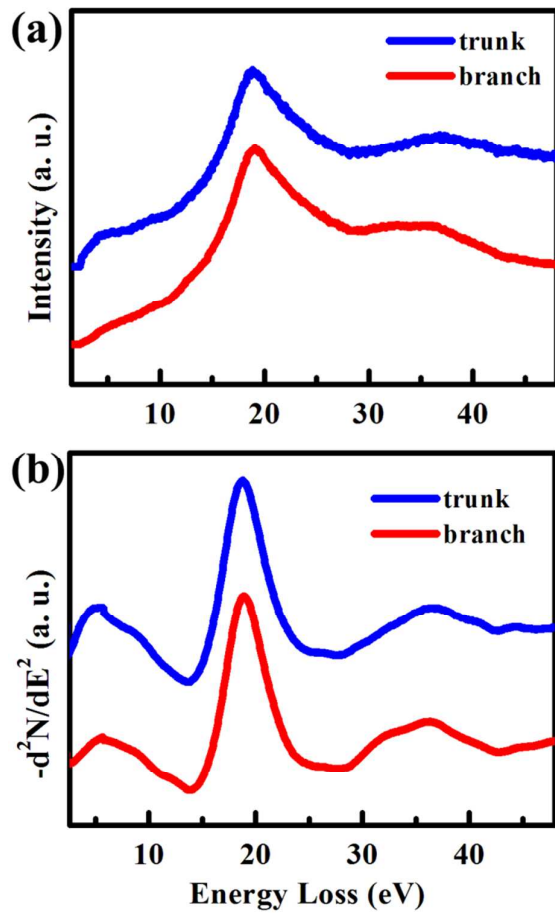


Figure 3 by L. L. Wu, et al.

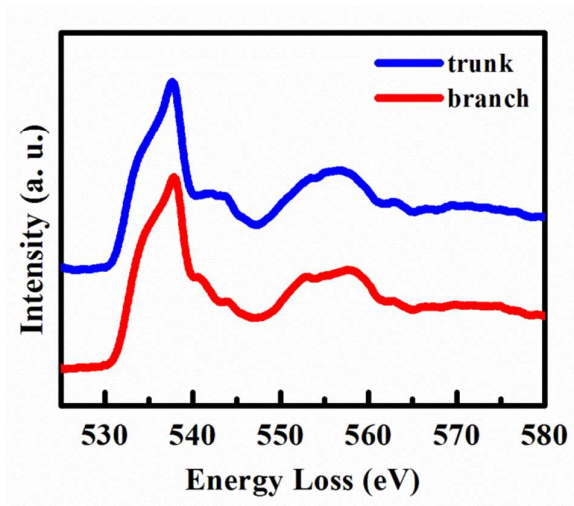


Figure 4 by L. L. Wu, et al.

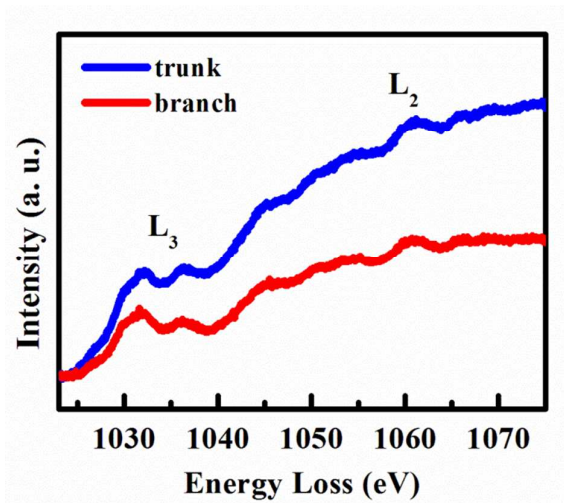


Figure 5 by L. L. Wu, et al.